

# An efficient and flexible approach for computing rovibrational polaritons from first principles

Tamás Szidarovszky\*

*Institute of Chemistry, ELTE Eötvös Loránd University,*

*H-1117 Budapest, Pázmány Péter sétány 1/A, Hungary*

arXiv:2304.02346v2 [physics.chem-ph] 6 Apr 2023

# Abstract

A theoretical framework is presented for the computation of rovibrational polaritonic states of a molecule in a lossless infrared (IR) microcavity. In the proposed approach the quantum treatment of the rotational and vibrational motion of the molecule can be formulated using arbitrary approximations. The cavity-induced changes in electronic structure are treated perturbatively, which allows using the existing polished tools of standard quantum chemistry for determining electronic molecular properties. As a case study, the rovibrational polaritons and related thermodynamic properties of H<sub>2</sub>O in an IR microcavity are computed for varying cavity parameters and applying various approximations to describe the molecular degrees of freedom. For small light-matter coupling strengths the self-dipole interaction and the molecular polarizability can be safely ignored, however, with increasing coupling strength these become essential for obtaining accurate rovibropolaritonic energy levels. As long as the rovibrational model is appropriate for describing the field-free molecule, the computed rovibropolaritonic properties can be expected to be accurate as well. Strong light-matter coupling between the radiation mode of an IR cavity and the rovibrational states of H<sub>2</sub>O lead to noticeable changes in the thermodynamic properties of the system, and these changes seem to be dominated by non-resonant interactions between the quantum light and matter.

## I. INTRODUCTION

As an alternative to interactions of molecules with intense laser fields, strong light-matter coupling can also be achieved by the confinement of molecules in microscale optical or plasmonic cavities. When the light-matter coupling is stronger than the loss of the cavity mode and the decay rates in the matter, the strong coupling regime is reached, leading to the formation of hybrid light-matter states, called polaritons [1–8]. The confined photonic modes of the cavity can efficiently couple with either electronic or vibrational molecular states, depending on the cavity mode wavelength. The formation of vibrational polaritons in infrared (IR) microcavities has received a great deal of attention [9–15], owing to the possibility of modifying thermal chemical reactions with vibrational polaritons. As detailed in the reviews cited above, the full understanding of the effects of vibrational strong coupling

---

\* [tamas.janos.szidarovszky@ttk.elte.hu](mailto:tamas.janos.szidarovszky@ttk.elte.hu)

and the formation of vibrational polaritons on chemical reactivity is a challenge yet to be tackled.

In addition, closely related to chemical reactivity, the spectroscopy of vibrational polaritons have also been studied both by means of experiments [16–25] and theory [26–35]. For examples, a detailed investigation of the vibrational polaritons of single anharmonic vibrational modes was carried out in Refs. [29, 30], while Ref. [31] showed the presence of unique optical nonlinearities of  $N$  anharmonic oscillators interacting with an IR cavity mode. Using a one-dimensional description Ref. [32] simulated various properties of anharmonic oscillators (OH, LiH, NH<sub>3</sub>), with coordinate dependent dipole functions, coupled to an IR photonic mode, from the weak to ultrastrong coupling regimes. Refs. [27, 28] provide empirically adjustable anharmonic approaches, which allow incorporating decay mechanisms. The method of vibrational configuration interaction (VCI) has also been implemented in the context of vibrational polaritons [33], and the vibropolaritonic energies and IR spectra of H<sub>2</sub>O molecules were computed.

Despite the cavity radiation being resonant with (ro)vibrational transitions, the radiation-induced changes in the electronic structure might also become important [34]. For IR cavities, in which the photon energy and respective frequency is comparable to those in rovibrational transitions, the molecule can be assumed to have an electronic structure adiabatically transformed by the radiation field, known as the cavity Born-Oppenheimer approximation (CBO) [36, 37]. To describe nuclear dynamics, CBO combines naturally with the QEDFT [38–40] and QEDCC [41] methods, whereby the effect of the cavity radiation is explicitly included in the electronic structure calculation, and the nuclear and photonic modes are governed by the resulting CBO potential energy surfaces. Using QEDFT and linear response theory, the vibrational polaritons of CO<sub>2</sub> and Fe(CO)<sub>5</sub> molecules could be computed from first principles [34].

In this work we present an alternative theoretical framework to compute the (ro)vibrational polaritons of molecules in a lossless IR microcavities. The proposed approach extends existing computational tools in three main ways: (1) the exact quantum treatment of molecular rotation is incorporated, which can be important considering that the coupling strength between the transition dipole and the radiation field, having laboratory-fixed polarization, depends on molecular orientation; (2) the cavity-induced changes in electronic structure are treated perturbatively, which allows using the existing efficient tools of standard quantum

chemistry and theoretical molecular spectroscopy to determine electronic molecular properties; and (3) various approximations and levels of theory regarding the description of the molecular degrees of freedom and light-matter interaction can be made. The flexibility of the proposed framework can be useful to arrange the appropriate balance between accuracy and computational effort, allowing it to be used for a wide range of molecules of various complexity.

## II. THEORETICAL FOUNDATIONS

### A. Rovibrational polaritons

The Hamiltonian of a molecule interacting with a single lossless cavity mode can be written in the dipole approximation as a sum of the field-free molecular rovibronic Hamiltonian ( $\hat{H}_m^{\text{tot}}$ ), the radiation mode Hamiltonian ( $\hat{H}_c$ ), the interaction term between the molecular dipole and the electric field of the radiation mode ( $-\hat{\mathbf{E}}_c \hat{\boldsymbol{\mu}}^{\text{tot}}$ ), and the self-dipole energy term ( $\hat{H}_{\text{sd}}$ ) [42, 43]

$$\begin{aligned} \hat{H} &= \hat{H}_m^{\text{tot}} + \hat{H}_c - \hat{\mathbf{E}}_c \hat{\boldsymbol{\mu}}^{\text{tot}} + \hat{H}_{\text{sd}} = \\ &\hat{H}_m^{\text{tot}} + \hbar\omega_c \hat{a}_c^\dagger \hat{a}_c - \sqrt{\frac{\hbar\omega_c}{\varepsilon_0 V}} \mathbf{e} \hat{\boldsymbol{\mu}}^{\text{tot}} (\hat{a}_c^\dagger + \hat{a}_c) + \frac{1}{2\varepsilon_0 V} (\mathbf{e} \hat{\boldsymbol{\mu}}^{\text{tot}})^2 = \\ &\hat{H}_m^{\text{tot}} + \hbar\omega_c \hat{a}_c^\dagger \hat{a}_c - g \mathbf{e} \hat{\boldsymbol{\mu}}^{\text{tot}} (\hat{a}_c^\dagger + \hat{a}_c) + \frac{g^2}{2\hbar\omega_c} (\mathbf{e} \hat{\boldsymbol{\mu}}^{\text{tot}})^2 \end{aligned} \quad (1)$$

where  $\hat{a}_c^\dagger$  and  $\hat{a}_c$  are photon creation and annihilation operators, respectively,  $\omega_c$  is the frequency of the cavity mode,  $\hbar$  is Planck's constant divided by  $2\pi$ ,  $\varepsilon_0$  is the electric constant,  $V$  is the volume of the electromagnetic mode,  $\mathbf{e}$  is the polarization vector of the cavity mode, and  $\hat{\boldsymbol{\mu}}^{\text{tot}}$  is the total dipole moment operator of the molecule. In the last line of Eq. (1) the coupling strength  $g = \sqrt{\hbar\omega_c/(\varepsilon_0 V)}$  was introduced.

As already mentioned in the introduction, for IR cavities, in which the photon energy is comparable to those in rovibrational transitions, the cavity-induced changes in the electronic structure can be incorporated into the CBO potential energy surfaces, which govern the nuclear and photonic degrees of freedom. In this work the effects of the cavity radiation on the electronic structure is accounted for perturbatively, using the electronic polarizability. Such a perturbative approach is common practice for electronically non-resonant laser fields of moderate intensity [44–48]. Therefore, for IR cavity radiations, being off resonant with the

electronic transitions, and for coupling strengths typically realized in experiments [21, 25], the perturbative treatment of electronic excitation seems to be a reasonable approach. Taking the expectation value of the Hamiltonian in Eq.(1) with the cavity-modified electronic wave function, and utilizing the standard approach [49] of expressing the modified dipole with the field-free permanent dipole  $\hat{\mu}_0$  and the first-order static polarizability  $\hat{\alpha}$ , both nuclear coordinate-dependent, one obtains the following rovibrophotonic Hamiltonian.

$$\begin{aligned} \hat{H} = & \hat{H}_{\text{rovib}} - g\mathbf{e}\hat{\mu}_0(\hat{a}_c^\dagger + \hat{a}_c) - \frac{g^2}{2}\mathbf{e}\hat{\alpha}\mathbf{e}(\hat{a}_c^\dagger + \hat{a}_c)(\hat{a}_c^\dagger + \hat{a}_c) + \hbar\omega_c\hat{a}_c^\dagger\hat{a}_c + \\ & + \frac{g^2}{2\hbar\omega_c}(\mathbf{e}\hat{\mu}_0)^2 + \frac{g^3}{4\hbar\omega_c}[(\mathbf{e}\hat{\mu}_0)(\mathbf{e}\hat{\alpha}\mathbf{e}) + (\mathbf{e}\hat{\alpha}\mathbf{e})(\mathbf{e}\hat{\mu}_0)](\hat{a}_c^\dagger + \hat{a}_c) + \frac{g^4}{8\hbar\omega_c}(\mathbf{e}\hat{\alpha}\mathbf{e})^2(\hat{a}_c^\dagger + \hat{a}_c)^2, \end{aligned} \quad (2)$$

where  $\hat{H}_{\text{rovib}}$  is the field-free rovibrational Hamiltonian utilizing the unperturbed electronic potential energy surface (PES). For the sake of simplicity, we omit the terms with  $g^3$  and  $g^4$  below (for the H<sub>2</sub>O molecule and cavity parameters investigated in this work, it was numerically tested that these terms are in fact negligible). To describe the rovibropolaritonic system, the  $|N\rangle|\Psi^{nJM}\rangle$  direct-product functions provide a complete basis, where the  $|\Psi^{nJM}\rangle$  field-free rovibrational eigenstates satisfy

$$\hat{H}_{\text{rovib}}|\Psi^{nJM}\rangle = E^{nJ}|\Psi^{nJM}\rangle, \quad (3)$$

$J$  and  $M$  are the rotational angular momentum and its projection onto the space-fixed  $z$ -axis, respectively,  $n$  is all other quantum numbers uniquely defining the rovibrational states, and  $|N\rangle$  is a photon number state of the cavity radiation. The matrix representation of Eq. (2) using the field-free rovibrational eigenstates  $|\Psi^{nJM}\rangle$  as molecular basis functions can be expressed conveniently by using the spherical basis representation of the molecular dipole and polarizability, which are obtained from the Cartesian representation as [50]  $\mu^{(1,0)} = \mu_3$ ,  $\mu^{(1,\pm 1)} = \frac{1}{\sqrt{2}}(\mp\mu_1 - i\mu_2)$ ,  $\alpha^{(0)} = -\frac{1}{\sqrt{3}}(\alpha_{11} + \alpha_{22} + \alpha_{33})$ ,  $\alpha^{(2,\pm 2)} = \frac{1}{2}[\alpha_{11} - \alpha_{22} \pm i(\alpha_{12} + \alpha_{21})]$ ,  $\alpha^{(2,\pm 1)} = \frac{1}{2}[\mp(\alpha_{13} + \alpha_{31}) - i(\alpha_{23} + \alpha_{32})]$ , and  $\alpha^{(2,0)} = \frac{1}{\sqrt{6}}(2\alpha_{33} - \alpha_{22} - \alpha_{11})$ . Assuming the cavity electric field to be polarized along the lab-fixed  $z$ -axis,  $\mathbf{e} = (0, 0, 1)$ , one obtains matrix elements of the following form

$$\begin{aligned}
& \langle N | \langle \Psi^{JMn} | \hat{H} | \Psi^{J'M'n'} \rangle | N' \rangle = E^{Jn} \delta_{JJ'} \delta_{nn'} \delta_{MM'} \delta_{NN'} \\
& -g \left( \sqrt{N'+1} \delta_{NN'+1} + \sqrt{N'} \delta_{NN'-1} \right) \sum_{k=-1}^1 \langle \Psi^{JMn} | D_{0k}^1 * \mu^{\text{BF},(1,k)} | \Psi^{J'M'n'} \rangle \\
& -\frac{g^2}{\sqrt{6}} \left( \sqrt{(N'+1)(N'+2)} \delta_{N,N'+2} + (2N'+1) \delta_{N,N'} + \sqrt{N'(N'-1)} \delta_{N,N'-2} \right) \times \\
& \quad \left[ \sum_{k=-2}^2 \langle \Psi^{JMn} | D_{0k}^2 * \alpha^{\text{BF},(2,k)} | \Psi^{J'M'n'} \rangle - \frac{1}{\sqrt{2}} \langle \Psi^{JMn} | \alpha^{\text{BF},(0)} | \Psi^{J'M'n'} \rangle \right] \\
& + \delta_{NN'} \delta_{MM'} \frac{g^2}{2\hbar\omega_c} \sum_{k,k'=-1}^1 \sum_{J'',n''} \langle \Psi^{JMn} | D_{0k}^1 * \mu^{\text{BF},(1,k)} | \Psi^{J''M''n''} \rangle \langle \Psi^{J''M''n''} | D_{0k'}^1 * \mu^{\text{BF},(1,k')} | \Psi^{J'M'n'} \rangle,
\end{aligned} \tag{4}$$

where the relation  $\sum_{J'',M'',n''} |\Psi^{J''M''n''}\rangle \langle \Psi^{J''M''n''}| = \hat{I}$  for the molecular state space was used. In the above equation the superscript BF stands for body-fixed components, i.e., those directly obtained from quantum chemistry computations, and  $D_{km}^j$  are the Wigner-D matrices [50] responsible for transforming the body-fixed spherical basis components of the molecular properties into their lab-fixed components (which are used to express the interaction with the cavity electric field in Eq.(2)). Using the general variational expansion  $|\Psi^{JMn}\rangle = \sum_{K,v} C_{Kv}^{Jn} |v\rangle |JKM\rangle$  for the field-free rovibrational eigenstates, where  $|v\rangle$  are vibrational basis functions and  $|JKM\rangle$  are the symmetric top rotational eigenstates [50], the terms containing the Wigner-D matrices in Eq. (4) can be evaluated as

$$\begin{aligned}
& \sum_{k=-1}^1 \langle \Psi^{JMn} | D_{0k}^1 * \mu^{\text{BF},(1,k)} | \Psi^{J'M'n'} \rangle = \\
& \sum_{k=-1}^1 \left( \sum_{v,v'} \langle v | \mu^{\text{BF},(1,k)} | v' \rangle \sum_{K,K'} C_{Kv}^{Jn} * C_{K'v'}^{J'n'} \langle JKM | D_{0k}^1 * | J'K'M' \rangle \right),
\end{aligned} \tag{5}$$

and

$$\begin{aligned}
& \sum_{k=-2}^2 \langle \Psi^{JMn} | D_{0k}^2 * \alpha^{\text{BF},(2,k)} | \Psi^{J'M'n'} \rangle - \frac{1}{\sqrt{2}} \langle \Psi^{JMn} | \alpha^{\text{BF},(0)} | \Psi^{J'M'n'} \rangle = \\
& \sum_{k=-2}^2 \left( \sum_{v,v'} \langle v | \alpha^{\text{BF},(2,k)} | v' \rangle \sum_{K,K'} C_{Kv}^{Jn} * C_{K'v'}^{J'n'} \langle JKM | D_{0k}^2 * | J'K'M' \rangle \right) \\
& - \delta_{JJ'} \delta_{MM'} \frac{1}{\sqrt{2}} \sum_{v,v'} \langle v | \alpha^{\text{BF},(0)} | v' \rangle \sum_K C_{Kv}^{Jn} * C_{Kv'}^{J'n'},
\end{aligned} \tag{6}$$

where  $\langle JKM | D_{0k}^{j*} | J'K'M' \rangle = (2J+1)^{1/2}(2J'+1)^{1/2}(-1)^{-k+M'-K'} \begin{pmatrix} J & j & J' \\ M & 0 & -M' \end{pmatrix} \begin{pmatrix} J & j & J' \\ K & -k & -K' \end{pmatrix}$ , which implies that  $M = M'$  for all non-zero matrix elements, as expected for a system with cylindrical symmetry. The  $k$ th rovibrational polaritonic  $|\Psi_{\text{pol}}^{k,M}\rangle$  eigenstate and  $E_{\text{pol}}^{k,M}$  energy are computed as the  $k$ th eigenvector and eigenvalue, respectively, of the Hamiltonian defined by Eq. (4).

The rovibrational polaritons of H<sub>2</sub>O molecules in an IR microcavity are simulated using two different molecular models and various approximations within each model. In the first molecular model, results of a high-accuracy variational rovibrational simulation are used for constructing the matrix elements in Eq. (4). This approach can be regarded as the theoretical benchmark within the framework utilized. The second molecular model is based on the harmonic oscillator and rigid-rotor (HORR) approximations [49], with all parameters taken from black-box quantum chemistry calculations. The second model aims to reveal the robustness and flexibility of the approach presented in this work, important for considering applications to larger systems.

### III. COMPUTATIONAL DETAILS

All results presented in this work are converged with respect to the size of the basis employed to construct the Hamiltonian in Eq. (4). The largest basis used includes a maximum photon number of two, and all rovibrational states with  $J \leq 10$  and an energy no more than 5500 cm<sup>-1</sup> above the zero point vibrational energy (ZPVE). Such parameters ensure that all vibrational fundamentals and the bending overtone of H<sub>2</sub>O, including rotationally excited states, are included in the basis. The two methods for obtaining the field-free molecular rovibrational eigenstates, to be used in the direct product basis employed in Eq. (4), are detailed below.

#### A. Molecular model I.

In the high-accuracy variational approach, the field-free, bound rovibrational eigenstates of H<sub>2</sub>O were computed using the D2FOPI protocol and program suite [51], with the PES of Ref. [52]. In these computations the C<sub>2v</sub>(M) molecular symmetry [49] was kept as described in Ref. [53]. In the D2FOPI program, the time-independent rovibrational Schrödinger

equation for a triatomic molecule is solved by an iterative eigensolver using symmetry adopted Wigner matrices [50] as rotational basis functions and a mixed discrete variable representation (DVR) [54] and finite basis representation [54] along the vibrational degrees of freedom expressed in the orthogonal Jacobi coordinate system.

For each irreducible representation of the  $C_{2v}(M)$  molecular symmetry group, the calculations included (1) a complete set of rotational basis functions, whose size varies depending on the given value of the  $J$  rotational quantum number, (2) 45 potential optimized (PO) spherical DVR basis functions [51] along the  $R_1 \equiv R(\text{H-H})$  coordinate, (3) 55 PO spherical DVR basis functions along the  $R_2 \equiv R(\text{O-H}_2)$  coordinate, connecting the O atom with the center of mass of the  $\text{H}_2$  moiety, and (4) 25 associated Legendre functions along the  $\theta$  angle coordinate defined by the direction of the two stretching coordinates. The coordinate ranges used in the calculations were  $R(\text{H-H})/\text{bohr} \in (0,10)$  and  $R(\text{O-H}_2)/\text{bohr} \in (0,6)$ , and the nuclear masses  $m_{\text{H}}=1.00727647$  u and  $m_{\text{O}}=15.990526$  u were employed.

With these parameters the D2FOPI computations provide the  $C_{Kv}^{Jn}$  rovibrational eigenvector coefficients (See Eqs. (5) and (6)) and the  $E^{Jn}$  rovibrational energies (Eq. (4)), all values used in this work converged to within  $0.01 \text{ cm}^{-1}$ . The obtained vibrational fundamentals are  $\tilde{\nu}_1 = 3657.05 \text{ cm}^{-1}$ ,  $\tilde{\nu}_2 = 1594.73 \text{ cm}^{-1}$ , and  $\tilde{\nu}_3 = 3796.99 \text{ cm}^{-1}$ . The dipole moment surfaces  $\mu^{\text{BF},(1,k)}(R_1, R_2, \theta)$  and the polarizability surfaces  $\alpha^{\text{BF},(0)}(R_1, R_2, \theta)$  and  $\alpha^{\text{BF},(2,k)}(R_1, R_2, \theta)$  were generated using the results of Refs. [55] and [56], respectively. The matrix elements  $\langle v | \mu^{\text{BF},k} | v' \rangle$  of Eq. (5) and  $\langle v | \alpha^{\text{BF},(2,k)} | v' \rangle$  and  $\langle v | \alpha^{\text{BF},(0)} | v' \rangle$  of Eq. (6) can be efficiently computed with the DVR basis employed in D2FOPI [46].

## B. Molecular model II.

The second molecular model employed in this work uses the HORR approximation, with molecular parameters obtained from black-box quantum chemistry computations, carried out with MOLPRO [57] on the gold standard CCSD(T)/aug-cc-pVQZ level [58, 59]. The obtained harmonic frequencies and rotational constants are  $\tilde{\nu}_1 = 3830.84 \text{ cm}^{-1}$ ,  $\tilde{\nu}_2 = 1649.72 \text{ cm}^{-1}$ ,  $\tilde{\nu}_3 = 3940.43 \text{ cm}^{-1}$ ,  $B_z = 14.5720 \text{ cm}^{-1}$ ,  $B_y = 9.4934 \text{ cm}^{-1}$  and  $B_x = 27.2393 \text{ cm}^{-1}$ , where the molecule is in the body-fixed xz plane, with the z-axis pointing towards the oxygen. The body-fixed  $\mu_i^{\text{BF}}(Q_1, Q_2, Q_3)$  dipole and  $\alpha_{i,j}^{\text{BF}}(Q_1, Q_2, Q_3)$  polarizability functions were expanded along the normal coordinates to second order, using finite differences to



compute their derivatives with respect to the normal coordinates, then transformed to the spherical representation for Eqs. (5-6). Due to this expansion along the normal coordinates, the matrix elements  $\langle v|\mu^{\text{BF},k}|v'\rangle$  of Eq. (5) and  $\langle v|\alpha^{\text{BF},(2,k)}|v'\rangle$  and  $\langle v|\alpha^{\text{BF},(0)}|v'\rangle$  of Eq. (6) can be determined with analytical formulae in the HO vibrational basis. In the HORR approximation the  $C_{Kv}^{Jn}$  expansion coefficients of Eqs. (5-6) simplify to  $C_K^{Jn}$ , and can be obtained by solving the RR problem in the  $|JKM\rangle$  rotational basis.

## IV. RESULTS AND DISCUSSION

### A. Rovibrational polaritonic energies

Figure 1 shows the computed eigenvalues of the Hamiltonian in Eq. (4) as a function of the  $g$  coupling strength, using the variational molecular eigenstates in the basis and a photon energy of  $1630\text{ cm}^{-1}$ , nearly resonant with the HOH bending fundamental, i.e., the  $(010)[111] \leftarrow (000)[000]$  rovibrational transition at  $1635.0\text{ cm}^{-1}$  (note that the  $\Delta J = 0$  purely vibrational transition is forbidden). The middle panels of Figure 1 were obtained by neglecting the self-dipole term from the Hamiltonian, while the right panels were generated by dropping the polarizability term as well. As seen in Figure 1, for small  $g$  values both molecular polarizability and the self-dipole interaction can be safely ignored, however, their effect can become significant for increasing  $g$ , and eventually higher-order polarizabilities might also need to be considered. Nonetheless, for currently relevant experimental coupling strengths [21, 25], the effect of the self-dipole and polarizability terms is rather small, the latter indicating that the perturbative inclusion of the cavity-induced changes in the electronic structure of the molecule is appropriate. Figure 1 also demonstrates that molecular energy shifts due to the light-matter interactions have a strong effect on polariton formation, as these level shifts can create or destroy the resonance condition between photon-excited or rovibrationally excited states. These generally negative energy shifts mean that in order to efficiently generate polaritons at low coupling strengths, the photon energy should be somewhat red shifted with respect to the field-free molecular transition. Figure 2 is the same as Figure 1, but with a photon energy of  $3690\text{ cm}^{-1}$  tuned to the symmetric OH stretching fundamental, i.e., the  $(100)[111] \leftarrow (000)[000]$  transition at  $3693.3\text{ cm}^{-1}$ .

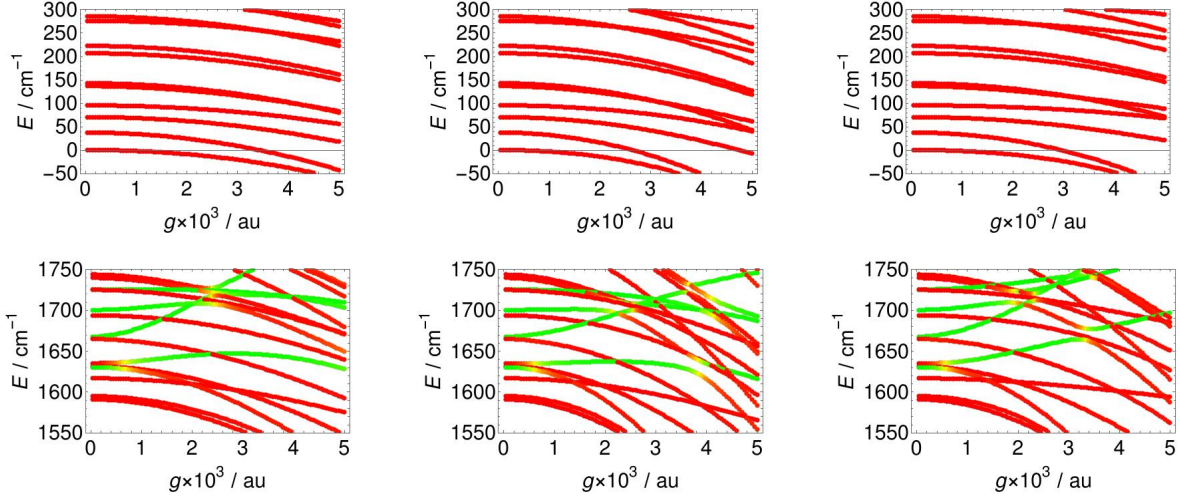


FIG. 1: Left panels: converged eigenvalues of the rovibronic Hamiltonian of Eq. (4) as a function of the  $g$  coupling strength, obtained using the numerically exact variational molecular eigenstate basis and a photon wave number of  $\tilde{\nu} = 1630 \text{ cm}^{-1}$ . Middle panels: same as in left panels, but with the self-dipole interaction neglected. Right panels: same as middle panels, but with the induced dipole (polarizability) interaction also neglected. The colors of the lines represent their character: red indicates zero expectation value for the photon number, while green represents one photon expectation value. Yellow indicates a mixture of photonic and material excitations.

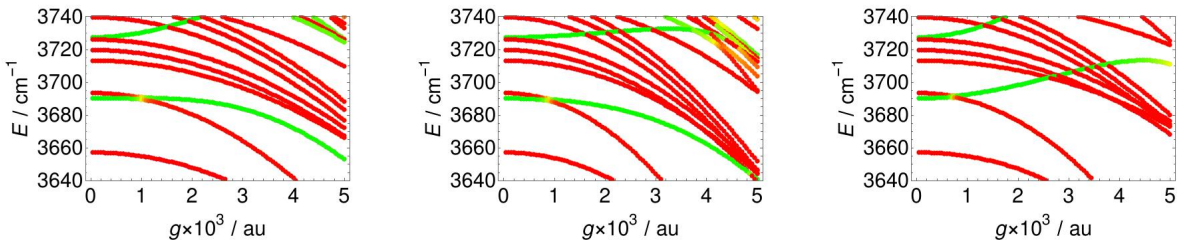


FIG. 2: Same as Figure 1, but with a photon wave number of  $\tilde{\nu} = 3690 \text{ cm}^{-1}$ .

Figure 3 presents the energy landscape for  $g = 0.001$  and  $g = 0.0025$  coupling strengths and varying photon energy near the HOH bending fundamental. In accordance with previous figures, for  $g = 0.001$  neglecting polarizability and self-dipole interactions is an accurate approximation, however, for the larger coupling strength of  $g = 0.0025$ , these interactions become important.

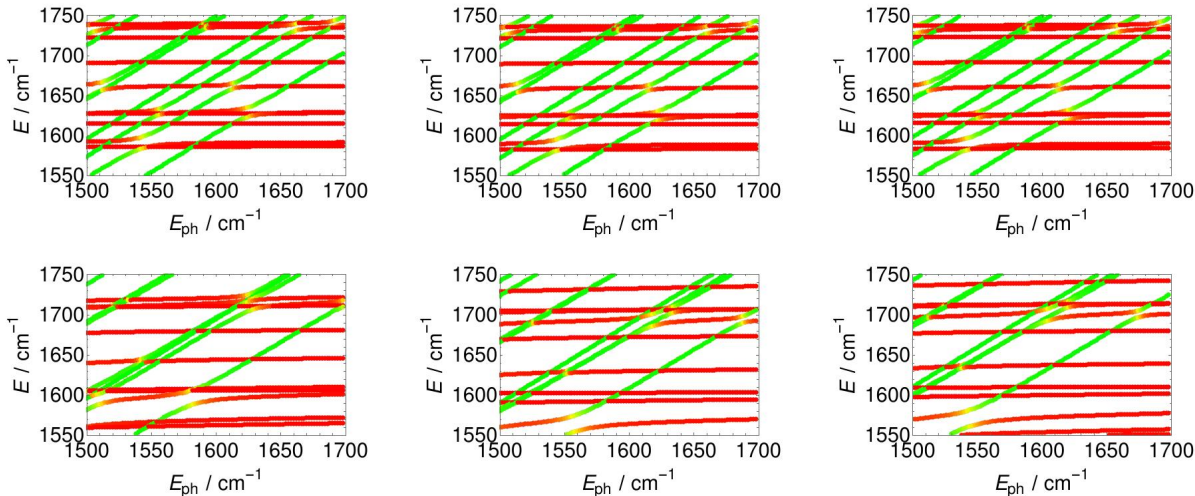


FIG. 3: Same as Figure 1, but the polaritonic energies are now expressed as a function of the  $E_{\text{ph}}$  cavity photon energy, at the coupling strengths of  $g = 0.001$  (upper row) and  $g = 0.0025$  (bottom row).

Figure (4) compares the rovibropolaritonic energies obtained using the two molecular models. As seen in the upper row and middle row panels, for the semi-rigid  $\text{H}_2\text{O}$  molecule, the HO approximation works remarkably well for describing the coupling strength-dependence of the polaritonic eigenstates correlating with the vibrational fundamentals. There is a shift in energy between the variational and HO vibrational fundamentals ( $51 \text{ cm}^{-1}$  in the upper row and  $174 \text{ cm}^{-1}$  in the middle row), which can be easily taken care of by scaling the HO force constants [60], a common procedure in theoretical molecular spectroscopy. In addition, several red lines can be seen, which are located differently with respect to the vibrational fundamentals in the two columns. These lines correspond to rotationally highly excited states, indicating that the tens of  $\text{cm}^{-1}$  differences observed are a consequence of the RR approximation breaking down for rotationally highly excited states, as expected. For low rotational excitations the two columns show nearly identical results, as presented by the

lower row of Figure 4. Overall, Figure 4 implies that if the HORR approach is suitable for a specific system under field-free conditions, then it should be suitable to describe the light contaminated states in the IR microcavity as well. Caution, however, is needed to make sure that the HORR approach is appropriate for the full energy range considered.

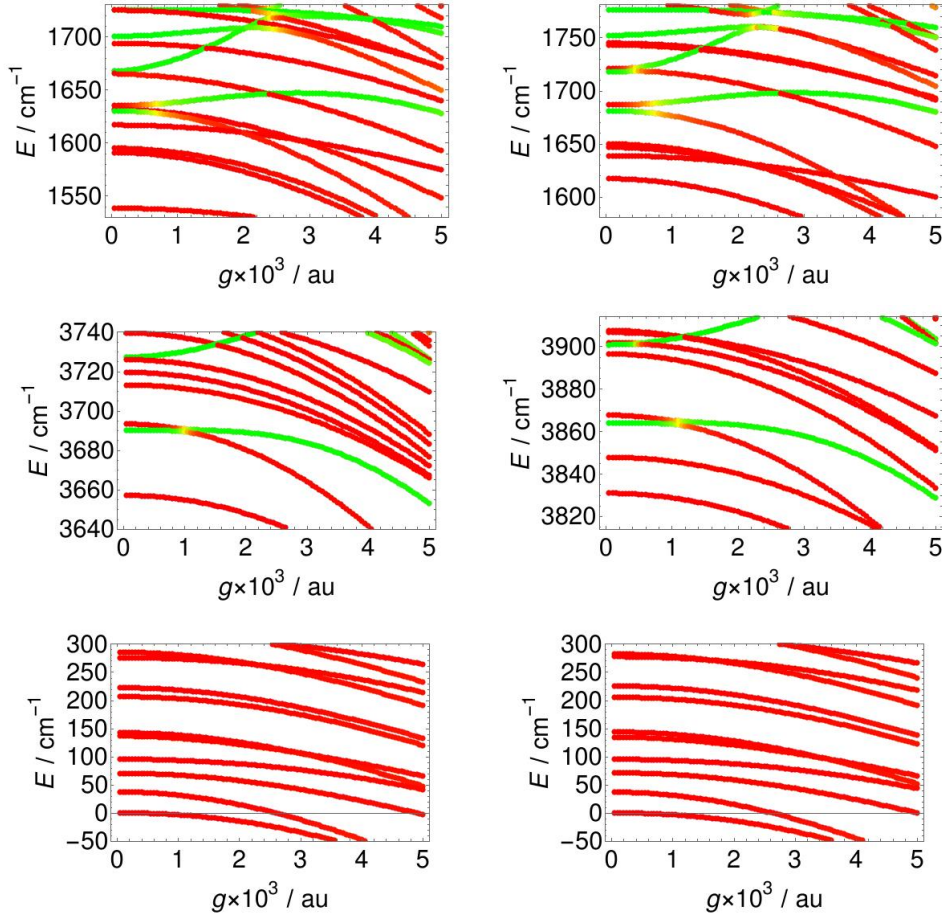


FIG. 4: Left column: converged eigenvalues of the rovibrophotonic Hamiltonian of Eq. (4) as a function of the  $g$  coupling strength, obtained using the numerically exact variational molecular eigenstate basis and photon wave numbers of  $\tilde{\nu} = 1630 \text{ cm}^{-1}$  (upper and lower panels) and  $\tilde{\nu} = 3690 \text{ cm}^{-1}$  (middle panel). Right column: same as in left column, but obtained using the HORR approximation for the molecular eigenstates and photon wave numbers of  $\tilde{\nu} = 1681 \text{ cm}^{-1}$  (upper and lower panels) and  $\tilde{\nu} = 3864 \text{ cm}^{-1}$  (middle panel).

## B. Thermochemistry of H<sub>2</sub>O in IR microcavities

With the rovibropolaritonic energy levels computed and available, one can construct the partition function and other thermochemical quantities of the “rovibrating H<sub>2</sub>O + IR cavity mode” system at different temperatures using the standard tools of thermochemistry [61]. In the following, results computed for ortho water are presented. Figure 5 shows various thermodynamic quantities presented as a function of temperature at different  $g$  coupling strengths for  $\tilde{\nu} = 1630 \text{ cm}^{-1}$  photon wave number. To highlight the changes induced by the light-matter coupling, Figure 5 also shows the changes in the various thermodynamic quantities with respect to the  $g = 0$  scenario. It can be seen in Figure 5 that light-matter interaction indeed changes the thermodynamic properties, and the temperature dependence of these changes is not trivial. In most cases the effect is less than a percent, although for the heat capacity it can reach around ten percent.

As expected from Figure 1 and shown in Figure 6, including molecular polarizability and the self-dipole interaction is necessary for obtaining quantitatively correct numbers, the permanent dipole-only model significantly overestimates the light-matter coupling-induced changes (compare right column of Fig. 5 with left column of Fig. 6). The right column of Figure 6 shows that when it comes the summation of energy levels at ambient temperatures, the HORR approach needs to be improved, as the cavity-induced changes in thermochemistry are underestimated in this case. Finally, Figure 7 shows how various thermodynamic quantities change with respect to the  $g = 0$  scenario, using a fixed  $g = 0.005$  value, presented as a function of temperature and for different  $\tilde{\nu}$  photon wave numbers near the HOH bending fundamental. Figure 7 demonstrates some systematic changes with respect to the photon wave number, but no resonance effect is apparent. This indicates that the efficient formation of rovibrational polaritons for specific vibrational modes does not dominate the thermochemistry in this case.

Overall, the computed results show that strong light-matter coupling between the radiation mode of an IR cavity and the rovibrational states of H<sub>2</sub>O lead to noticeable changes in the thermodynamic properties of the system, and these changes seem to be dominated by non-resonant interactions between light and matter. The computed changes in thermochemistry induced by the light-matter interaction seem to be sensitive to the accuracy of the rovibrophotonic energy levels.

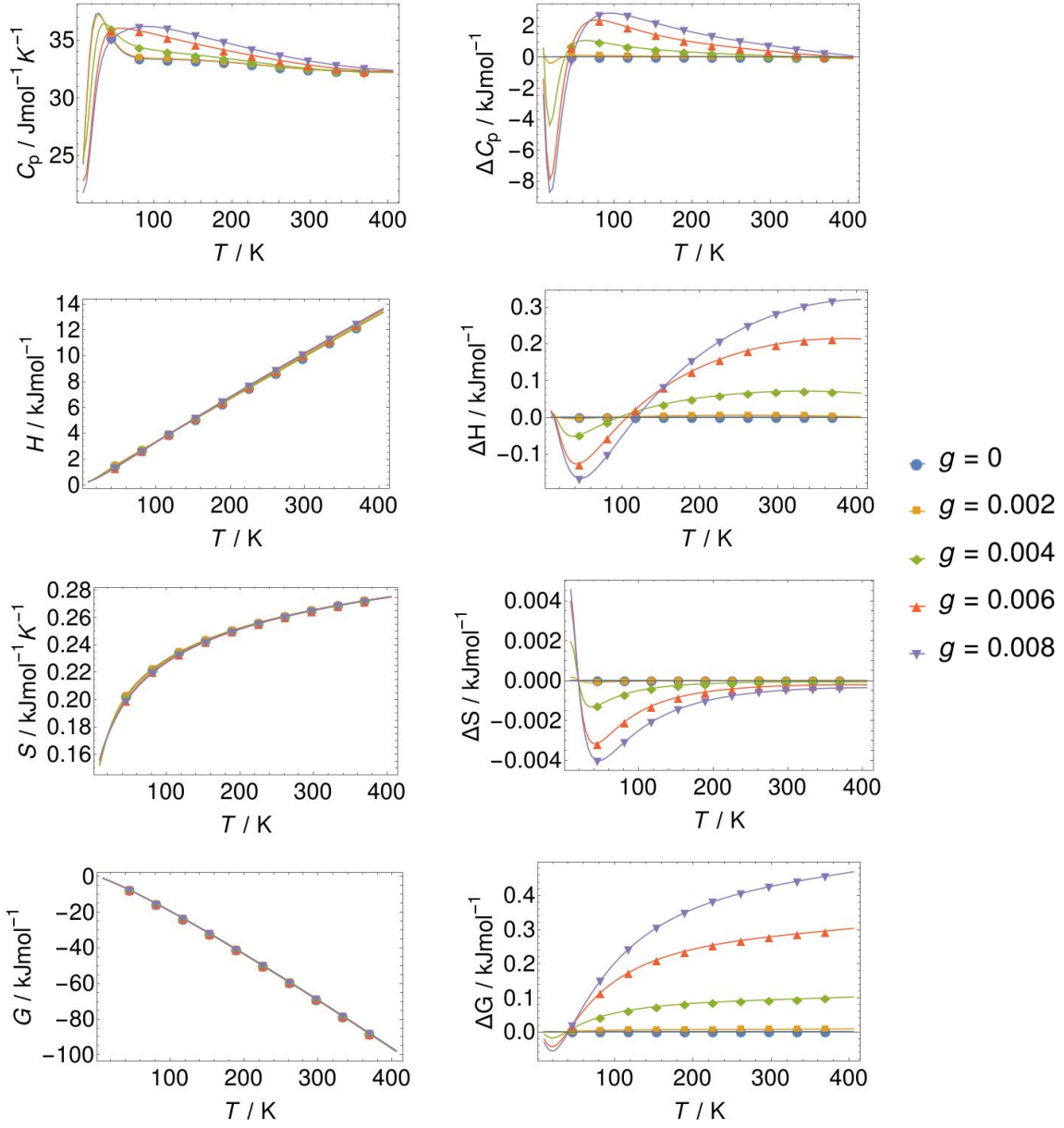


FIG. 5: Various thermodynamic quantities presented as a function of temperature using  $\tilde{\nu} = 1630 \text{ cm}^{-1}$  and different  $g$  coupling strengths (left column), and the changes in the various thermodynamic quantities with respect to the  $g = 0$  scenario.



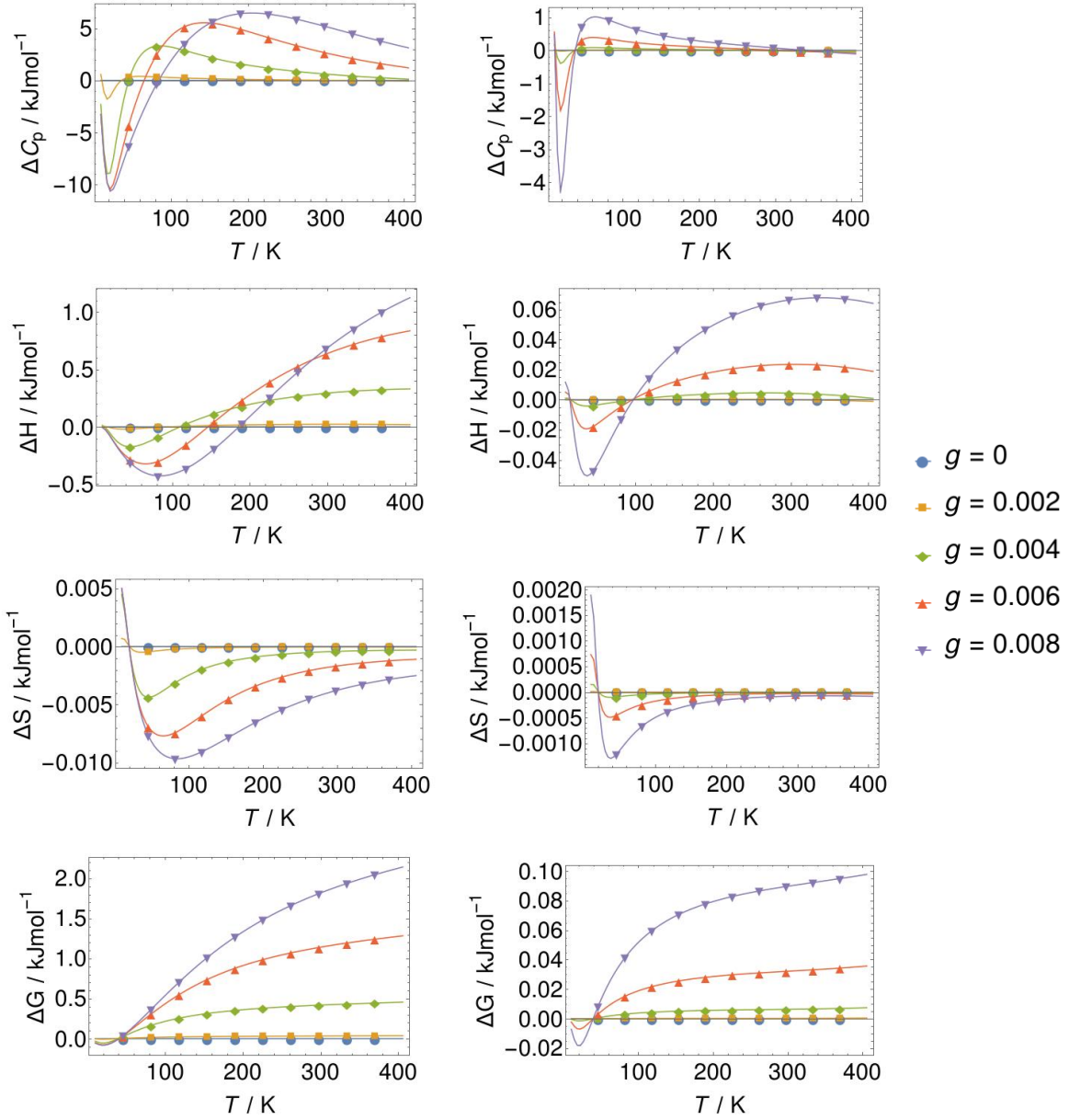


FIG. 6: Changes in the various thermodynamic quantities with respect to the  $g = 0$  scenario. Left column:  $\tilde{\nu} = 1630 \text{ cm}^{-1}$ , using the variational molecular basis, self dipole and polarizability interaction terms neglected. Right column:  $\tilde{\nu} = 1681 \text{ cm}^{-1}$ , using the HORR molecular basis and the full Hamiltonian of Eq. (4).

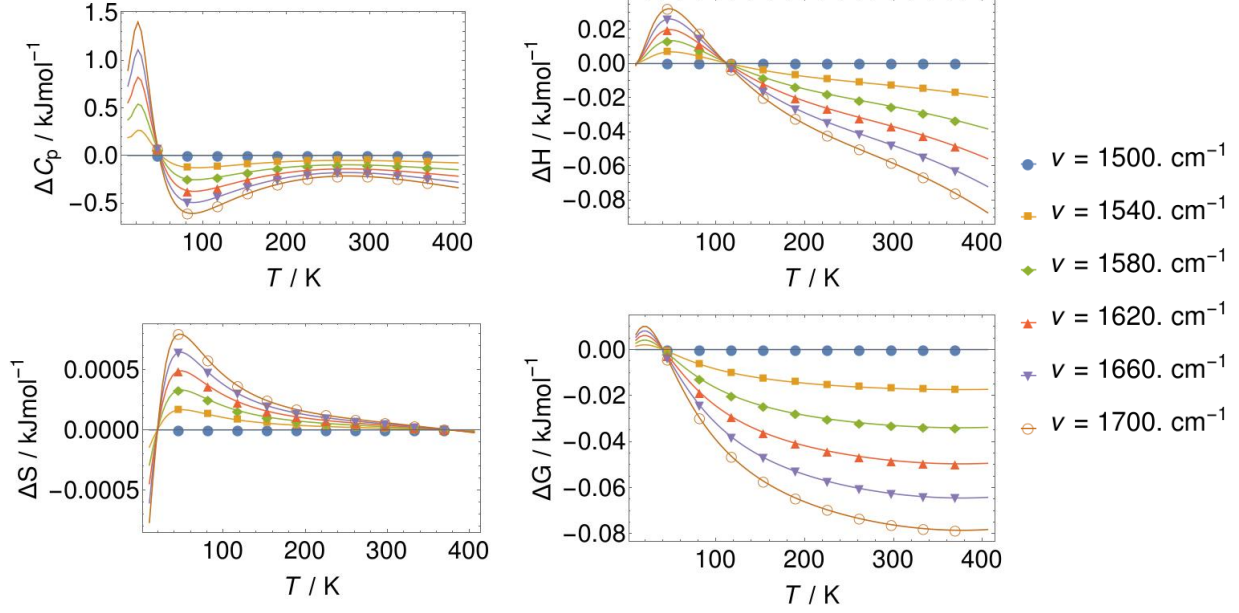


FIG. 7: Changes in the thermodynamic quantities with respect to the  $\tilde{\nu} = 1500 \text{ cm}^{-1}$  scenario using the full Hamiltonian of Eq. (4) with a fixed  $g = 0.005$  value, presented as a function of temperature for different  $\tilde{\nu}$  photon wave numbers near the HOH bending fundamental (exact resonance for  $(010)[111] \leftarrow (000)[000]$  is at  $1635.0 \text{ cm}^{-1}$ ).

Thermodynamics is in principle applicable to macroscopic amounts of molecules, therefore, it is a further issue how the results presented here are related to the realistic mesoscopic systems with many water molecules collectively interacting with the radiation mode. This question is left for future work.



## V. SUMMARY

(1) A new theoretical framework was presented for the computation of molecular rovibrational polaritons in a lossless infrared (IR) cavity, in which the quantum description of molecular rotation and vibration which can be formulated using arbitrary approximations. The molecular parameters required by the proposed approach can be obtained from standard quantum chemistry tools, circumventing the need to rely on theoretical methods which explicitly incorporate the cavity radiation for determining molecular electronic properties. The validity of the presented framework is justified as long as the light-induced changes in the electronic structure can be treated perturbatively, i.e., through molecular polarizabilities. For current experimental setups on vibrational polaritons, this seems to be the case.

(2) The rovibrational polaritons of  $\text{H}_2\text{O}$  were computed using different molecular models and considering the impact of different terms in the Hamiltonian of Eq. (4). (2.1) Due to the light-induced energy shift of the molecular energy levels, resonance condition and the formation of polaritons is determined by the coupling strength and the photon energy simultaneously. The energy shifts are dominantly negative, meaning that ensuring the resonance condition at low coupling strengths requires somewhat red shifted photon energies. (2.2) With increasing coupling strength  $g$ , the effects of the self-dipole interaction and the molecular polarizability increase, and need to be accounted for to obtain accurate rovibropolaritonic energy levels. (2.3) For  $\text{H}_2\text{O}$  and in the investigated energy range the HORR approximation performs well in describing rovibropolaritonic properties, indicating that as long as the rovibrational model is appropriate for describing the field-free molecule, the computed rovibropolaritonic properties can be expected to be accurate as well.

(3) Thermochemical quantities were computed from the rovibropolaritonic energy levels of  $\text{H}_2\text{O}$ . (3.1) It was found that strong light-matter coupling between the radiation mode of an IR cavity and the rovibrational states of  $\text{H}_2\text{O}$  lead to noticeable changes in the thermodynamic properties of the system, and these changes seems to be dominated by non-resonant interactions between light and matter. (3.2) Special care should be given to the accuracy of the rovibropolaritonic energy levels if the cavity-induced changes in thermochemistry are to be computed.

## VI. ACKNOWLEDGEMENTS

This research was supported by the János Bolyai Research Scholarship of the Hungarian Academy of Sciences and by the ÚNKP-22-5 New National Excellence Program of the Ministry for Innovation and Technology from the source of the National Research, Development and Innovation Fund. The Author is also grateful to NKFIH for additional support (Grant No. FK134291).

- 
- [1] T. W. Ebbesen, Hybrid Light-Matter States in a Molecular and Material Science Perspective, *Acc. Chem. Res.* **49**, 2403 (2016).
  - [2] R. F. Ribeiro, L. A. Martínez-Martínez, M. Du, J. Campos-Gonzalez-Angulo, and J. Yuen-Zhou, Polariton chemistry: controlling molecular dynamics with optical cavities, *Chem. Sci.* **9**, 6325 (2018).
  - [3] J. Feist, J. Galego, and F. J. Garcia-Vidal, Polaritonic Chemistry with Organic Molecules, *ACS Photonics* **5**, 205 (2018).
  - [4] R. Chikkaraddy, B. de Nijs, F. Benz, S. J. Barrow, O. A. Scherman, E. Rosta, A. Demetriadou, P. Fox, O. Hess, and J. J. Baumberg, Single-molecule strong coupling at room temperature in plasmonic nanocavities, *Nature* **535**, 127 (2016).
  - [5] F. Herrera and F. C. Spano, Cavity-controlled chemistry in molecular ensembles, *Phys. Rev. Lett.* **116**, 238301 (2016).
  - [6] M. Hertzog, M. Wang, J. Mony, and K. Börjesson, Strong light-matter interactions: a new direction within chemistry, *Chemical Society Reviews* **48**, 937 (2019).
  - [7] F. Herrera and J. Owrutsky, Molecular polaritons for controlling chemistry with quantum optics, *The Journal of Chemical Physics* **152**, 100902 (2020).
  - [8] M. Kowalewski and S. Mukamel, Manipulating molecules with quantum light, *Proceedings of the National Academy of Sciences* **114**, 3278 (2017).
  - [9] K. Hirai, J. A. Hutchison, and H. Uji-i, Recent progress in vibropolaritonic chemistry, *ChemPlusChem* **85**, 1981 (2020).
  - [10] K. Nagarajan, A. Thomas, and T. W. Ebbesen, Chemistry under vibrational strong coupling, *Journal of the American Chemical Society* **143**, 16877 (2021).

- [11] B. S. Simpkins, A. D. Dunkelberger, and J. C. Owrutsky, Mode-specific chemistry through vibrational strong coupling (or a wish come true), *The Journal of Physical Chemistry C* **125**, 19081 (2021).
- [12] D. S. Wang and S. F. Yelin, A roadmap toward the theory of vibrational polariton chemistry, *ACS Photonics* **8**, 2818 (2021).
- [13] D. Sidler, M. Ruggenthaler, C. Schäfer, E. Ronca, and A. Rubio, A perspective on ab initio modeling of polaritonic chemistry: The role of non-equilibrium effects and quantum collectivity, *The Journal of Chemical Physics* **156**, 230901 (2022).
- [14] T. E. Li, B. Cui, J. E. Subotnik, and A. Nitzan, Molecular polaritonics: Chemical dynamics under strong light–matter coupling, *Annual Review of Physical Chemistry* **73**, 43 (2022).
- [15] A. D. Dunkelberger, B. S. Simpkins, I. Vurgaftman, and J. C. Owrutsky, Vibration-cavity polariton chemistry and dynamics, *Annual Review of Physical Chemistry* **73**, 429 (2022).
- [16] A. Shalabney, J. George, H. Hiura, J. A. Hutchison, C. Genet, P. Hellwig, and T. W. Ebbesen, Enhanced raman scattering from vibro-polariton hybrid states, *Angewandte Chemie International Edition* **54**, 7971 (2015).
- [17] R. Damari, O. Weinberg, D. Krotkov, N. Demina, K. Akulov, A. Golombek, T. Schwartz, and S. Fleischer, Strong coupling of collective intermolecular vibrations in organic materials at terahertz frequencies, *Nature Communications* **10**, 3248 (2019).
- [18] B. Xiang, R. F. Ribeiro, M. Du, L. Chen, Z. Yang, J. Wang, J. Yuen-Zhou, and W. Xiong, Intermolecular vibrational energy transfer enabled by microcavity strong light–matter coupling, *Science* **368**, 665 (2020).
- [19] Z. Yang, B. Xiang, and W. Xiong, Controlling quantum pathways in molecular vibrational polaritons, *ACS Photonics* **7**, 919 (2020).
- [20] B. Xiang, R. F. Ribeiro, Y. Li, A. D. Dunkelberger, B. S. Simpkins, J. Yuen-Zhou, and W. Xiong, Manipulating optical nonlinearities of molecular polaritons by delocalization, *Science Advances* **5** (2019).
- [21] B. Xiang, R. F. Ribeiro, A. D. Dunkelberger, J. Wang, Y. Li, B. S. Simpkins, J. C. Owrutsky, J. Yuen-Zhou, and W. Xiong, Two-dimensional infrared spectroscopy of vibrational polaritons, *Proceedings of the National Academy of Sciences* **115**, 4845 (2018).
- [22] A. D. Dunkelberger, B. T. Spann, K. P. Fears, B. S. Simpkins, and J. C. Owrutsky, Modified relaxation dynamics and coherent energy exchange in coupled vibration-cavity polaritons,

- Nature Communications **7**, 13504 (2016).
- [23] A. B. Grafton, A. D. Dunkelberger, B. S. Simpkins, J. F. Triana, F. J. Hernández, F. Herrera, and J. C. Owrutsky, Excited-state vibration-polariton transitions and dynamics in nitroprusside, Nature Communications **12**, 214 (2021).
- [24] W. M. Takele, L. Piatkowski, F. Wackenhut, S. Gawinkowski, A. J. Meixner, and J. Waluk, Scouting for strong light-matter coupling signatures in raman spectra, Physical Chemistry Chemical Physics **23**, 16837 (2021).
- [25] A. D. Wright, J. C. Nelson, and M. L. Weichman, Rovibrational polaritons in gas-phase methane, Journal of the American Chemical Society **145**, 5982 (2023).
- [26] A. Strashko and J. Keeling, Raman scattering with strongly coupled vibron-polaritons, Physical Review A **94**, 023843 (2016).
- [27] P. Saurabh and S. Mukamel, Two-dimensional infrared spectroscopy of vibrational polaritons of molecules in an optical cavity, The Journal of Chemical Physics **144**, 124115 (2016).
- [28] R. F. Ribeiro, A. D. Dunkelberger, B. Xiang, W. Xiong, B. S. Simpkins, J. C. Owrutsky, and J. Yuen-Zhou, Theory for nonlinear spectroscopy of vibrational polaritons, The Journal of Physical Chemistry Letters **9**, 3766 (2018).
- [29] F. J. Hernández and F. Herrera, Multi-level quantum rabi model for anharmonic vibrational polaritons, The Journal of Chemical Physics **151**, 144116 (2019).
- [30] J. F. Triana, F. J. Hernández, and F. Herrera, The shape of the electric dipole function determines the sub-picosecond dynamics of anharmonic vibrational polaritons, The Journal of Chemical Physics **152**, 234111 (2020).
- [31] R. F. Ribeiro, J. A. Campos-Gonzalez-Angulo, N. C. Giebink, W. Xiong, and J. Yuen-Zhou, Enhanced optical nonlinearities under collective strong light-matter coupling, Physical Review A **103**, 063111 (2021).
- [32] E. W. Fischer and P. Saalfrank, Ground state properties and infrared spectra of anharmonic vibrational polaritons of small molecules in cavities, The Journal of Chemical Physics **154**, 104311 (2021).
- [33] Q. Yu and S. Hammes-Schiffer, Multidimensional quantum dynamical simulation of infrared spectra under polaritonic vibrational strong coupling, The Journal of Physical Chemistry Letters **13**, 11253 (2022).

- [34] J. Bonini and J. Flick, Ab initio linear-response approach to vibro-polaritons in the cavity born–oppenheimer approximation, *Journal of Chemical Theory and Computation* **18**, 2764 (2022).
- [35] T. Szidarovszky, P. Badankó, G. J. Halász, and Á. Vibók, Nonadiabatic phenomena in molecular vibrational polaritons, *The Journal of Chemical Physics* **154**, 064305 (2021).
- [36] J. Flick, M. Ruggenthaler, H. Appel, and A. Rubio, Atoms and molecules in cavities, from weak to strong coupling in quantum-electrodynamics (QED) chemistry, *Proceedings of the National Academy of Sciences* **114**, 3026 (2017).
- [37] J. Flick, H. Appel, M. Ruggenthaler, and A. Rubio, Cavity born–oppenheimer approximation for correlated electron–nuclear-photon systems, *Journal of Chemical Theory and Computation* **13**, 1616 (2017).
- [38] I. V. Tokatly, Time-dependent density functional theory for many-electron systems interacting with cavity photons, *Physical Review Letters* **110**, 10.1103/physrevlett.110.233001 (2013).
- [39] M. Ruggenthaler, J. Flick, C. Pellegrini, H. Appel, I. V. Tokatly, and A. Rubio, Quantum-electrodynamical density-functional theory: Bridging quantum optics and electronic-structure theory, *Physical Review A* **90**, 012508 (2014).
- [40] J. Malave, A. Ahrens, D. Pitagora, C. Covington, and K. Varga, Real-space, real-time approach to quantum-electrodynamical time-dependent density functional theory, *The Journal of Chemical Physics* **157**, 194106 (2022).
- [41] T. S. Haugland, E. Ronca, E. F. Kjørstad, A. Rubio, and H. Koch, Coupled cluster theory for molecular polaritons: Changing ground and excited states, *Physical Review X* **10**, 041043 (2020).
- [42] C. Cohen-Tannoudji, J. Dupont-Roc, and G. Grynberg, *Atom-Photon Interactions: Basic Processes and Applications*, Weinheim (Wiley-VCH Verlag GmbH and Co. KGaA, 2004).
- [43] V. Rokaj, D. M. Welakuh, M. Ruggenthaler, and A. Rubio, Light–matter interaction in the long-wavelength limit: no ground-state without dipole self-energy, *Journal of Physics B: Atomic, Molecular and Optical Physics* **51**, 034005 (2018).
- [44] H. Stapelfeldt and T. Seideman, Colloquium: Aligning molecules with strong laser pulses, *Rev. Mod. Phys.* **75**, 543 (2003).
- [45] C. P. Koch, M. Lemesko, and D. Sugny, Quantum control of molecular rotation, *Rev. Mod. Phys.* **91**, 035005 (2019).

- [46] T. Szidarovszky and K. Yamanouchi, Full-dimensional simulation of the laser-induced alignment dynamics of  $\text{H}_2\text{He}^+$ , *Molecular Physics* **115**, 1916 (2017).
- [47] T. Szidarovszky, M. Jono, and K. Yamanouchi, LIMA0: Cross-platform software for simulating laser-induced alignment and orientation dynamics of linear-, symmetric- and asymmetric tops, *Comp. Phys. Commun.* **228**, 219 (2018).
- [48] I. Simkó, K. Chordiya, A. G. Császár, M. U. Kahaly, and T. Szidarovszky, A quantum-chemical perspective on the laser-induced alignment and orientation dynamics of the  $\text{CH}_3\text{X}$  ( $\text{X} = \text{F}, \text{Cl}, \text{Br}, \text{I}$ ) molecules, *Journal of Computational Chemistry* **43**, 519 (2022).
- [49] P. R. Bunker and P. Jensen, *Molecular Symmetry and Spectroscopy* (NRC Research Press, Ottawa, 2006).
- [50] R. N. Zare, *Angular Momentum: Understanding Spatial Aspects in Chemistry and Physics* (Wiley, New York, 1988).
- [51] T. Szidarovszky, A. G. Császár, and G. Czakó, On the efficiency of treating singularities in triatomic variational vibrational computations. The vibrational states of  $\text{H}_3^+$  up to dissociation, *Phys. Chem. Chem. Phys.* **12**, 8373 (2010).
- [52] O. L. Polyansky, A. A. Kyuberis, N. F. Zobov, J. Tennyson, S. N. Yurchenko, and L. Lodi, ExoMol molecular line lists XXX: A complete high-accuracy line list for water, **480**, 2597 (2018).
- [53] T. Szidarovszky and A. G. Császár, Low-lying quasibound rovibrational states of  $\text{H}_2^{16}\text{O}$ , **111**, 2131 (2013).
- [54] J. C. Light and T. Carrington, Discrete variable representations and their utilization, **114**, 263 (2000).
- [55] L. Lodi, J. Tennyson, and O. L. Polyansky, A global, high accuracy ab initio dipole moment surface for the electronic ground state of the water molecule, *The Journal of Chemical Physics* **135**, 034113 (2011).
- [56] G. Avila, Ab initio dipole polarizability surfaces of water molecule: Static and dynamic at 514.5nm, *The Journal of Chemical Physics* **122**, 144310 (2005).
- [57] MOLPRO website, last accessed on April 7, 2023.
- [58] K. Raghavachari, G. W. Trucks, J. A. Pople, and M. Head-Gordon, A fifth-order perturbation comparison of electron correlation theories, *Chem. Phys. Lett.* **157**, 479 (1989).

- [59] T. H. Dunning Jr., Gaussian basis sets for use in correlated molecular calculations. I. The atoms boron through neon and hydrogen, *J. Chem. Phys.* **90**, 1007 (1989).
- [60] P. Pulay, G. Fogarasi, G. Pongor, J. E. Boggs, and A. Vargha, Combination of theoretical ab initio and experimental information to obtain reliable harmonic force constants. scaled quantum mechanical (QM) force fields for glyoxal, acrolein, butadiene, formaldehyde, and ethylene, *Journal of the American Chemical Society* **105**, 7037 (1983).
- [61] T. Furtenbacher, T. Szidarovszky, J. Hraby, A. A. Kyuberis, N. F. Zobov, O. L. Polyansky, J. Tennyson, and A. G. Császár, Definitive ideal-gas thermochemical functions of the  $\text{H}_2^{16}\text{O}$  molecule, **45**, 043104 (2016).